Microsc. Microanal. 21, 164–171, 2015
doi:10.1017/S1431927614013324

Microscopy AND Microanalysis

© MICROSCOPY SOCIETY OF AMERICA 2014

Effects of Preheating and Cooling Durations on Roll-to-Roll Hot Embossing

Seyoung Kim,* Youngsu Son, Heechang Park, Byungin Kim, and Dongwon Yun

Department of Robotics and Mechatronics, Korea Institute of Machinery & Materials (KIMM), 156 Gajeongbuk-Ro, Yuseong-Gu, Daejeon 305-343, South Korea

Abstract: In this study, we examined the sensitivity of embossed pattern depth to preheat supply and cooling and investigated how the pattern type and density affect the embossed depth. The main factors that affect embossed pattern qualities of roll-to-roll hot embossing, such as roller temperature, roller speed, and applied force, were determined using the response surface methodology. Eight conditions were then added to determine the time-dependent effects of heat transfer with custom-designed preheating and cooling systems. An extended preheat time for the polymethylmethacrylate substrate contributed to the significant change in the embossed depth, whereas the substrate-cooling did not exhibit a clear increasing or decreasing trend. Larger embossed depths were achieved in the horizontal patterns with lower density than in the vertical patterns, and the lower pattern densities showed greater embossed depths in most embossing conditions. We expect that this result will help to understand the effects of the pre- and posttreatment of roll-to-roll hot embossing by employing time duration factors of heat transfer, depending on the mold pattern type and density.

Key words: roll-to-roll hot embossing, preheating, cooling, pattern type, pattern density, pattern depth ratio

Introduction

Roll-to-roll (R2R) hot embossing makes fine structures on the surface of flexible polymer substrates [e.g., polymethylmethacrylate (PMMA) and polyethyleneterephthalate] by patterning the polymer with appropriate heat transfer, above its glass transition temperature, and pressing force. As hot roller embossing has the advantages of larger area and faster speed compared with hot plate embossing, it has been widely accepted as a mass-production method that can reproduce a broad range of industrial products including microfluidic devices, flexible electronics, flexible panel displays, microlens arrays, and many decorative applications (Chang et al., 2006; Fagan et al., 2009; Yeo et al., 2009, 2010).

However, the reduction in force holding time is an inherent disadvantage (i.e., causing polymer reflows), which can result in a reduction in embossed pattern quality (He et al., 2007; Ahn & Guo, 2008; Cho et al., 2009). This potential disadvantage can be partially compensated by optimizing the embossing parameters. Therefore, an optimum design of the embossing condition is necessary to replicate high quality patterns using R2R hot embossing.

There are a number of factors (operating parameters) that influence the pattern quality of R2R embossing, including roller temperature, roller speed, and applied force, which are generally considered as major factors. In practice, actual operating parameters were determined via process optimization or simple trial and error methods (Yeo et al., 2009, 2010; Velten et al., 2010; Liu et al., 2012).

Received March 19, 2014; accepted September 16, 2014
*Corresponding author. seyoungkim@kimm.re.kr

The effects of changing process parameters on embossed pattern qualities have been reported in microfabrication technology (e.g., hot roller embossing) (Ishizawa et al., 2008; Ng & Wang, 2008; Fagan et al., 2009; Yeo et al., 2009, 2010; Liu et al., 2012). However, the parameter studies were typically carried out under extremely limited conditions because finding globally optimal parameters for the highest pattern quality is difficult. For example, individual parameters, such as roller temperature and applied force, were sequentially changed from low to high values, and embossed pattern depths were tracked in every case, while other process parameters were selected discretionally and maintained constant during the experiments (Schift et al., 2006; Shan et al., 2010; Velten et al., 2010; Metwally et al., 2011).

Design of experiment techniques have often been used to examine the influence of individual process parameters on the corresponding microfabrication and to optimize all related parameters (Nouraei & Roy, 2009; Yeo et al., 2010; Lou et al., 2013; Omar et al., 2013). The Box–Behnken experimental design for hot roller embossing was employed to investigate the relationship between input process parameters on normalized pattern depth (Yeo et al., 2010). Optimal process parameters that maximize the output response were estimated by three-dimensional (3D) response surface methodology (RSM) (Nouraei & Roy, 2009; Yeo et al., 2010; Lou et al., 2013; Omar et al., 2013). However, the number of process parameters for the optimization was limited to three factors (e.g., roll temperature, preheat temperature, and applied pressure) because the addition of an input parameter can drastically increase the number of experimental trials (Myers et al., 2009).

In this study, we examined the sensitivity of embossed pattern depth to preheat supply and cooling and investigated

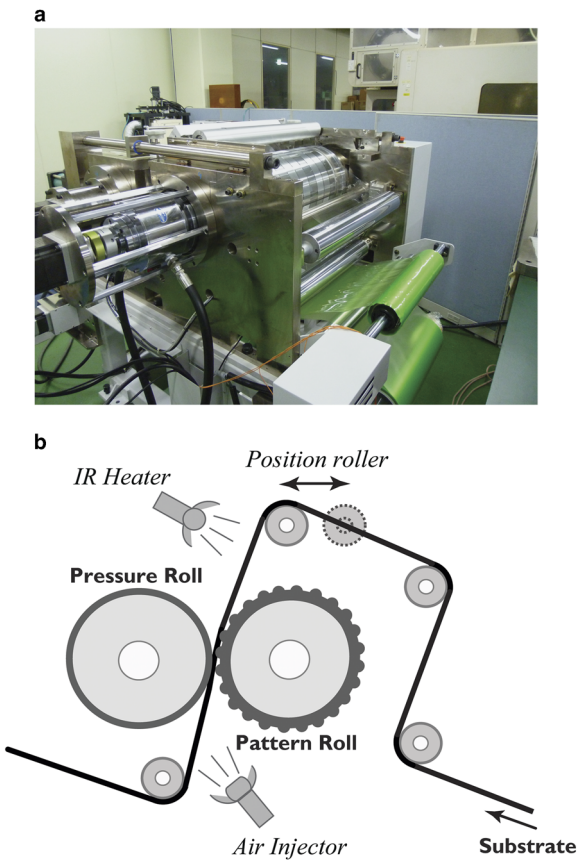

Figure 1. a: Lab-scale roll-to-roll hot embossing equipment. **b:** Schematic of the roll-to-roll hot embossing process including position roller, infrared heater, and custom-designed air injector.

how the pattern type and density affect the embossed depth. First, the optimization parameters for R2R hot embossing were classified into two categories, main factors and peripheral factors, because there are simply too many parameters that need to be considered. The main factors that affect embossed pattern qualities of R2R hot embossing, such as roller temperature, roller speed, and applied force, were determined using the RSM. Thereafter, eight conditions were added to determine the time duration effects of heat transfer with custom-designed preheating and cooling systems. Second, comparative studies were performed to better understand the effects of time-dependent parameters on hot roller embossing based on the experimental results.

Methods

R2R Hot Embossing Equipment

A lab-scale R2R embossing system was used in this study (Figs. 1a, 1b). Two rolls having the same radius, one for patterning (i.e., the pattern roll) and the other for pressuring (i.e., the pressure roll), were placed horizontally and powered by servomotors to rotate at the same speed but in the opposite direction. The rotational axis of the pattern roll was mounted on the frame, and the pressure roll was

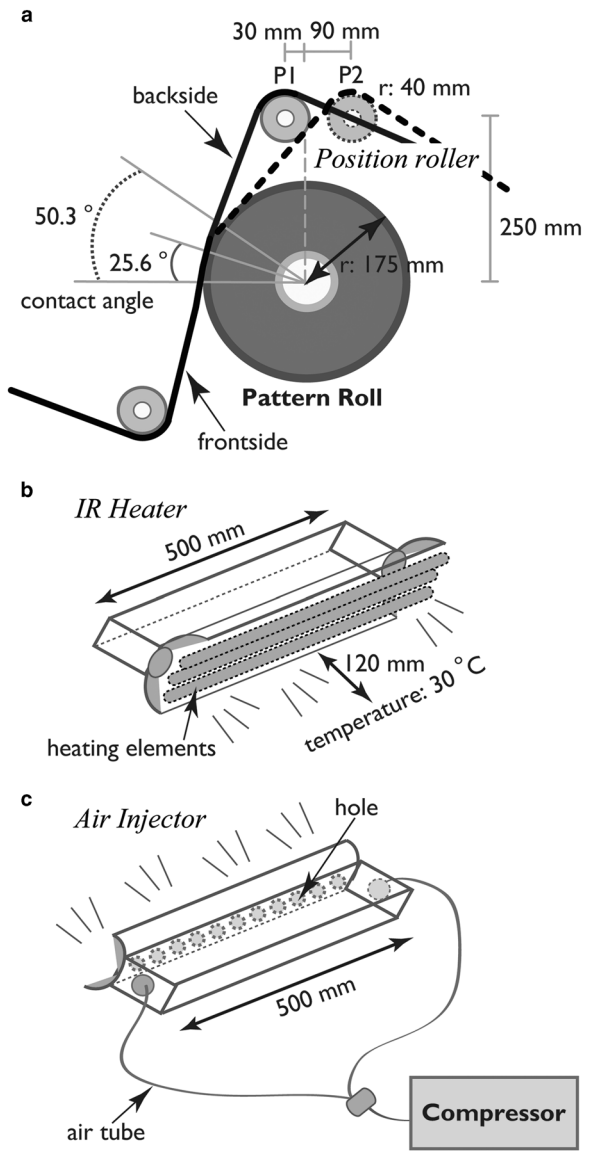

Figure 2. Detailed schematic of the (**a**) position roller, (**b**) infrared heater, and (**c**) air injector.

guided to move in a straight line toward the pattern roll by an electro-hydraulic system. The surface temperature of each roll was adjusted with a closed-loop temperature control based on the induction heating technique (Davies & Simpson, 1979; Erickson, 1995; Yun et al., 2012). The position roller that was placed above the pattern roll adjusted the contact length between the pattern roll and the polymer substrate by changing its horizontal position; therefore, a larger amount of preheat could be transferred to the front side of the PMMA substrate when started (Fig. 2a). An electric infrared heater (IR heater) preheated the backside of the polymer substrate before an embossing (Fig. 2b), whereas a custom-designed air injector cooled the polymer substrate immediately after the embossing (Fig. 2c). PMMA (C200; SEJIN T.S., Anseong, Korea) with a thickness of 80 μm was used as a substrate material for the R2R hot embossing process.

Mold and Pattern Specifications

The film mold (500 mm width) was fabricated via chrome plating methods after the copper-coated roll surface was laser patterned. A fiber laser with a mean laser power of 40 W was employed to carve micropatterns on the roll surface having a copper plating thickness of 300 μm. After engraving, the roller was cleaned and degreased to eliminate any particles, dirt, or residue. Then, the roller was placed in a series of tanks that were filled with an electrolyte solution in order to bind a thin plate of chromium onto the surface. With the release of electrical currents, the plating started to attach to the roll surface with uniform thickness of 1 μm determined by the length of exposure time. In the final stage of chrome plating, mold features with a height difference of about 3 μm along the length direction of the pattern roll were obtained.

The mold features consisted of horizontal and vertical striped patterns with constant line width (20 μm) and height (20 μm) (Figs. 3a, 3b). Each pattern type was composed of three pattern densities, 10, 33, and 50%, with different pitch widths, where the pattern density (PD) was calculated as follows (Fig. 3c):

$$\mathrm{PD} = \frac{\mathrm{line}}{\mathrm{pitch}} \times 100\,\%\,. \tag{1}$$

Experimental Protocol for R2R Hot Embossing

The RSM was employed to optimize the main factors that mostly affect embossed pattern qualities of R2R hot embossing, such as roller temperature, roller speed, and applied force. After we completed all of the experimental runs, the pattern roll temperature, pressure roll temperature, rolling speed, and applied force were set to 105°C (glass transition temperature of PMMA, $T_g \approx 105$°C), 30°C, 0.5 m/min, and 7 kN, respectively (Table 1), where the averaged embossed pattern depth had a maximum value. Although the pattern roll temperature and applied force for the maximum values were slightly different from the selected values, depending on pattern type and PD, differences in the embossed depth were <10%.

To examine the time duration effects of heat supply on the embossed pattern depth, eight conditions listed in Table 1 were tested with custom-designed preheating and cooling systems (Figs. 2a–2c). The position roller increased the contact angle from 25.6 to 50.3° (Fig. 2a), resulting in an increase in contact time from 9.3 to 18.4 s under the given roller speed (0.5 m/min). A contact duration exceeding 20 s forced the PMMA substrate out of shape because there is a limit on the level of preheating time beyond which the polymer may be excessively softened. The IR heater applied preheat (30°C; same as the pressure roll temperature) to the backside of the polymer substrate before embossing (Fig. 2b), whereas the embossed patterns were rapidly cooled to 21°C (room temperature) in just a few seconds when the air injector was switched on (Fig. 2c).

Pattern Depth Measurement and Data Analysis

Embossed pattern profiles were captured by a 3CCD real color confocal microscope (OPTELICS H1200; Lasertec, Yokohama, Japan), and depth measurements were reconfirmed by a surface roughness tester (SJ-301; Mitutoyo, Kawasaki, Japan). The depth measurements, average of maximum peak depths at three different points, were used to calculate the pattern depth ratio (PdR), which was defined as follows:

$$\mathrm{PdR} = \frac{d_{\mathrm{embossed}}}{h_{\mathrm{mold}}} \times 100\,\%\,. \tag{2}$$

where d_{embossed} and h_{mold} are the embossed depth on the substrate and the pattern height on the mold structure, respectively. The differences in PdR corresponding to each R2R hot embossing condition were tested with a two-sample t-test with a level of significance of $p < 0.05$.

Results

Sensitivity of PdR to Preheat Supply and Cooling

An extended preheating time between the pattern roll and PMMA substrate contributed to the increasing PdR (Figs. 4a, 4e). The increase in PdR was especially prominent in patterns with a density of 33%. This increasing trend was also observed in conditions considering the interaction effect (Fig. 5a).

The preheat supply to the substrate backside facing the pressure roll significantly contributed to the drops in PdR (Figs. 4a, 4b), but the statistical significance becomes weaker when the interaction terms are taken into account (Fig. 5b).

Overall, the custom-designed air injector was not effective in increasing PdR (Figs. 4a, 4c, and 5c). Although they considerably shortened the cooling time of the polymer immediately after an embossing, the shapes of the embossed patterns were not clearly different for both on–off conditions, which indicates that the reflow behavior of the polymer substrate was not altered. Only horizontal patterns with a density of 10% showed a statistically significant increase (Fig. 5c).

Pattern Type and PD Effects

Larger embossed depths were achieved in horizontal patterns with lower densities (Fig. 4 and Table 2). The horizontal patterns with densities of 10 and 33% showed greater embossed depths than the vertical patterns with densities of 10 and 33% ($p < 0.05$); however, the horizontal patterns with the highest density (50%) showed smaller depths than the vertical patterns with the same density.

The lower PD showed the larger embossed depth in most embossing conditions (Fig. 4 and Table 2). Horizontal patterns with a density of 10% showed the largest embossed depths, whereas overall depths of vertical patterns with densities of 10 and 33% showed greater embossed depths than a density of 50% in cases where the position roller was on, but the differences were not significant. This inversely proportional relationship between the PD and the embossed

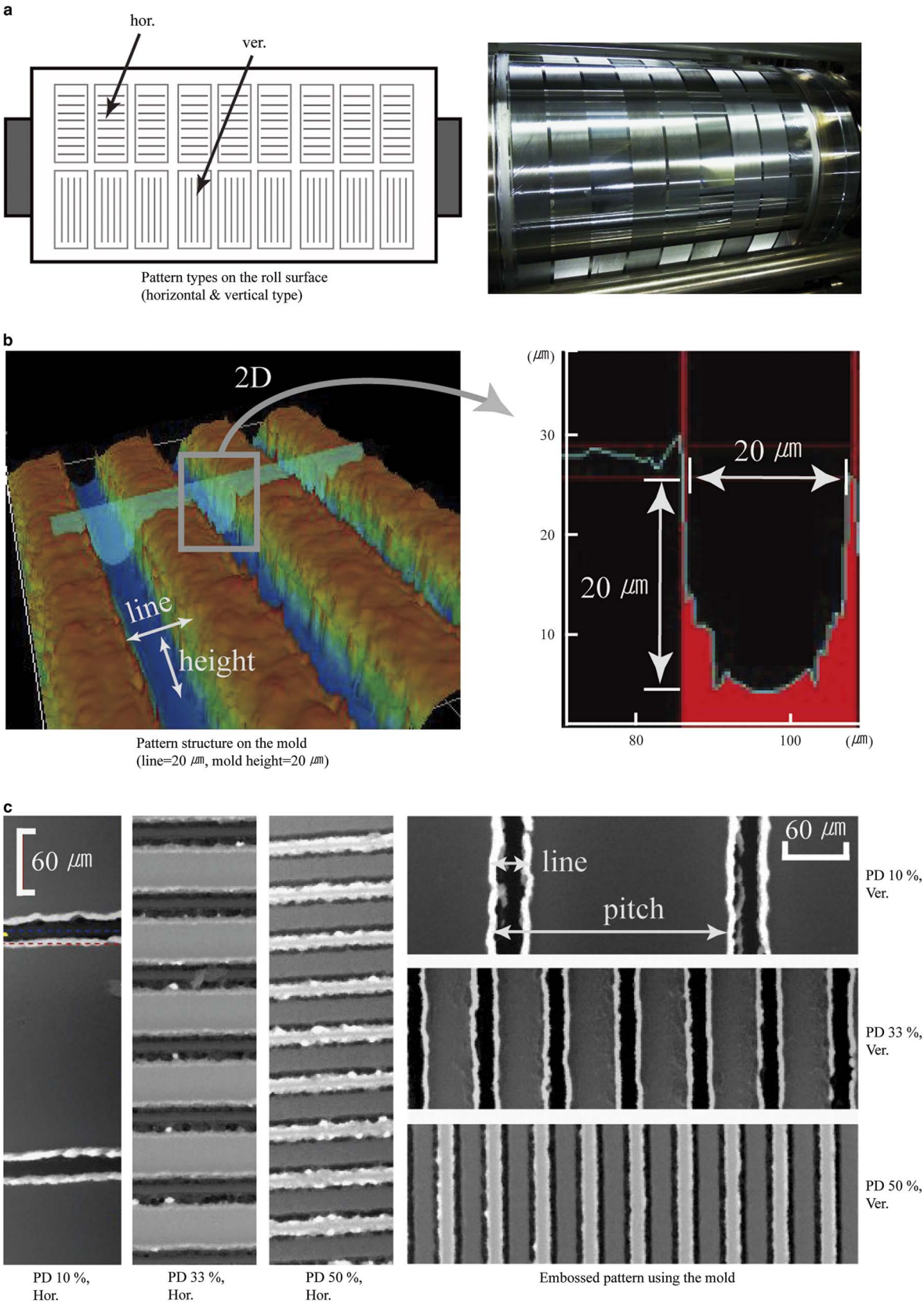

Figure 3. **a:** Horizontal and vertical pattern types on the surface of pattern roll, (**b**) two-dimensional (2D) and 3D pattern structures of the film mold captured by a 3D laser scanning microscope (VK-X100, Keyence, Osaka, Japan), (**c**) embossed patterns with density of 10, 33, and 50% captured by a 3CCD real color confocal microscope.

Table 1. Experimental Protocols of Roll-to-Roll Hot Embossing Process.

	Pattern Roll °C	Pressure Roll °C	Roll Speed m/min	Load kN	Position Roller on/off	IR Heater on/off	Air Injector on/off
Cond 1	105	30	0.5	7	off	off	off
Cond 2	105	30	0.5	7	off	on	off
Cond 3	105	30	0.5	7	off	off	on
Cond 4	105	30	0.5	7	off	on	on
Cond 5	105	30	0.5	7	on	off	off
Cond 6	105	30	0.5	7	on	on	off
Cond 7	105	30	0.5	7	on	off	on
Cond 8	105	30	0.5	7	on	on	on

pattern depth was more clearly observed in the horizontal pattern data.

Discussion

Preheat Time for the PMMA Substrate Contributed to the Significant Change in Embossed Depths

A longer contact time between the hot pattern roll and polymer substrate provoked sufficient heat transfer before an embossing, which most likely enhanced the polymer viscosity, resulting in an increase in pattern depth (Yeo et al., 2009, 2010). The time-dependent effects of heat transfer during the preheating stage are also important for pattern qualities and should be considered as tuning parameters, in addition to main factors such as roller temperature, roller speed, and applied force. Among these main factors for R2R hot embossing, the roller speed is also related to the time duration effects of heat transfer. A slower roller speed properly secures a longer contact time between mold and polymer, improving embossing results (Ng & Wang, 2008; Shan et al., 2008). However, the substrate's reverse side against the pressure roll might be better left untreated instead of being preheated because it needs to be more solid to provide proper support for the greater polymer deformation. Therefore, the pressure roll temperature may not be seriously considered as part of the optimization parameters because the optimal selection of the pressure roll temperature was near room temperature and its duration was ineffective in increasing pattern quality. Instead, we could include preheating parameters such as preheating temperature and preheating duration as major process parameters for hot roller embossing (Fagan et al., 2009; Yeo et al., 2009, 2010; Velten et al., 2010).

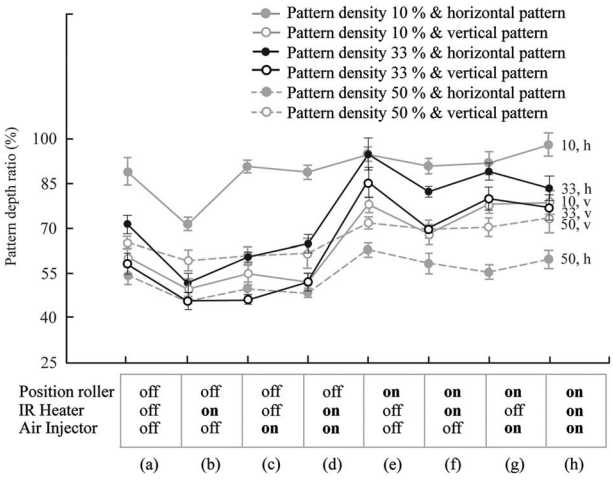

Figure 4. Sensitivity of pattern depth ratio (PdR) to preheat supply and cooling. The *X*-axis represents embossing conditions with combinations of preheating and cooling, while *Y*-axis represents PdRs. Error bars indicate standard deviations.

Differences in Contact Shape Corresponding to Pattern Type and Density Caused Unequal Levels of Flow Constraint

Horizontal mold patterns, which are perpendicular to the rolling direction, are likely to have more continuous polymer flow during the embossing stage than those for the vertical patterns, possibly because the less dense pattern along the roller nip provided less resistance to the material flow (Yeo et al., 2009, 2010). However, when the PD increased to 50% there were no advantages (Fig. 4 and Table 2). In previously published work performed by other groups (Yeo et al., 2009), the averaged embossed depths of horizontal patterns were found to be larger than those of vertical patterns, but the discrepancies were reduced and deviations were finally overlapped as PD increased.

Flexibility of the polymer behavior may be closely related to the PD (Schulz et al., 2003). Higher PD is thought to have constrained material flow, whereas lower PD allowed the polymer to be more pliable (Yeo et al., 2009, 2010). Simulation (i.e., the finite element multi-physics code *GOMA*) demonstrated that when patterns are sufficiently dense, constrained flow occurs, resulting in the reduced embossing performance (Rowland et al., 2005*a*; Rowland et al., 2005*b*). According to the simulation, constrained single-peak flow occurs when approximately half of the pattern height on the mold is greater than the cavity half width (i.e., $\frac{h_{\text{mold}}}{2} \geq \frac{\text{pitchline}}{2}$), nearly equivalent to the PD of 50% in our study. Simply put, differences in the contact shape

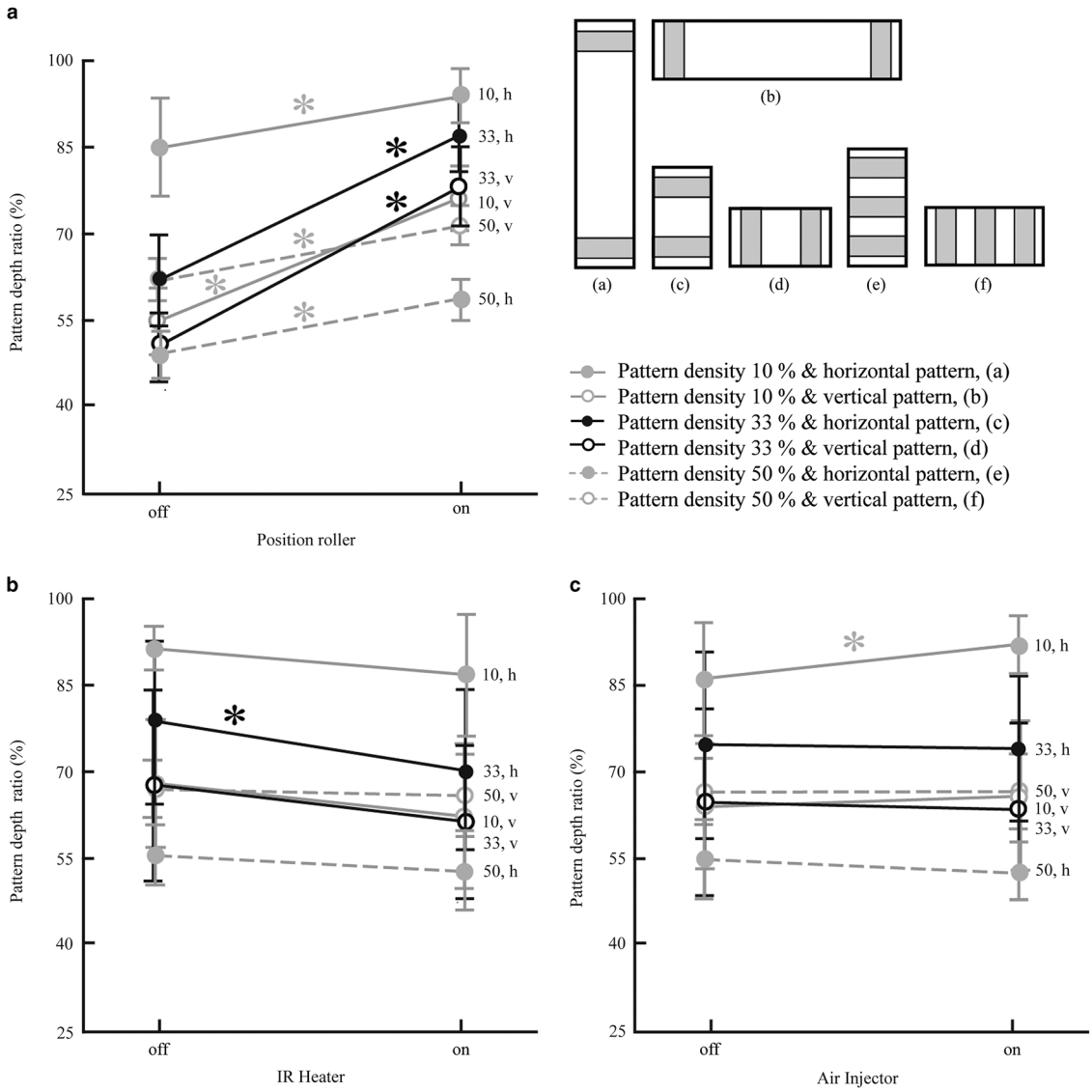

Figure 5. Effects of preheat supply and cooling on embossed pattern depth ratio (PdR) when the interaction terms are being accounted for. **a:** Effects of extended preheat time for the front side of the polymethylmethacrylate substrate, (**b**) effects of extended preheat time for the backside of the polymer substrate, (**c**) effects of shortened cooling time for the polymer substrate after an embossing. *Statistical significance is $p < 0.05$.

between the pattern roll and polymer substrate would cause unequal levels of flow constraint depending on the mold PD (Fig. 6), resulting in the discrepancies of embossed depths. Consequently, the lower PD is considered to have comparative advantages in terms of material flow behavior; in some cases (e.g., in Fig. 4) the PdRs of 33% vertical pattern

Table 2. Statistical Test for Differences in Pattern Depth Ratio Corresponding to Pattern Type and Density.

		Horizontal			Vertical		
Pattern Type	Pattern Density (%)	10	33	50	10	33	50
Horizontal	10		←	←	←	←	←
	33	↑		←		←	
	50	↑	↑		↑		↑
Vertical	10	↑		←			
	33	↑	↑				
	50	↑		←			

An arrow indicates the significance ($p < 0.05$ in more than seven conditions; Table 1), and the arrow's direction indicates the larger side.

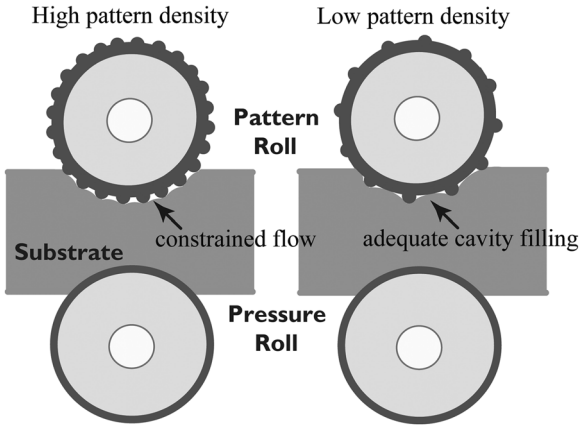

Figure 6. Schematic deformation profiles of unequal levels of flow constraint depending on the mold pattern density caused by differences in contact shape between pattern roll and polymer substrate.

(33, v) were slightly larger than those of 10% vertical pattern (10, v), but the deviations were largely overlapped under the conditions. In addition, the PdRs of 10% vertical pattern (10, v) were also smaller than those of 50% vertical pattern (50, v) in conditions a–d in Fig. 4, but the trends changed when the position roller was switched on for sufficient heat transfer (e.g., and h in Fig. 4). However, it is still difficult to clarify the combined effects of pattern type and density on the PdR because the PdRs of 10% vertical pattern (10, v) were smaller than those of 33% horizontal pattern (33, h) across all the embossing conditions.

Methodological Limitations

The optimization parameters for R2R hot embossing were classified into two categories, main factors and peripheral factors, because there are simply too many parameters that need to be considered. First, the main factors that mostly affect embossed pattern qualities, such as roller temperature, roller speed, and applied force, were selected based on the RSM. Second, the peripheral factors, such as preheating and cooling durations, were determined by testing eight conditions (Table 1) to fine-tune the time-dependent parameters related to the heat transfer. Although concluding whether the globally optimal parameters were obtained with the suggested protocols is difficult, we expect to be able to find one of the local maxima (i.e., locally maximum PdR) with less time and effort with the given equipment.

Future Perspectives

Experimental protocols need to be subdivided into various stages beyond an on–off switch to clearly understand the effects of time-dependent parameters on hot roller embossing. In addition, the cooling system needs to be redesigned with an entirely new interface or a different cooling element to examine the effectiveness in different ways. There might be a new cooling mechanism that would effectively control the thermal reflow of the PMMA substrate during a cooling process.

Acknowledgments

This research was supported by the research fund of the Korea Institute of Machinery & Materials (NK179E). The authors thank Sungwon Lee for his contribution to data collection.

References

Ahn, S.H. & Guo, L.J. (2008). High-speed roll-to-roll nanoimprint lithography on flexible plastic substrates. *Adv Mater* **20**(11), 2044–2049.

Chang, C., Yang, S. & Sheh, J. (2006). A roller embossing process for rapid fabrication of microlens arrays on glass substrates. *Microsyst Technol* **12**(8), 754–759.

Cho, Y., Kwon, S., Seo, J.-W., Kim, J.-G., Cho, J.-W., Park, J.-W., Kim, H. & Lee, S. (2009). Development of large area nano imprint technology by step and repeat process and pattern stitching technique. *Microelectron Eng* **86**(12), 2417–2422.

Davies, J. & Simpson, P. (1979). *Induction Heating Handbook*. New York, NY: McGraw-Hill.

Erickson, C.J. (1995). *Handbook of Electrical Heating for Industry*. Piscataway, NJ: IEEE Press.

Fagan, M.D., Kim, B.H. & Yao, D. (2009). A novel process for continuous thermal embossing of large-area nanopatterns onto polymer films. *Adv Polym Tech* **28**(4), 246–256.

He, Y., Fu, J.-Z. & Chen, Z.-C. (2007). Research on optimization of the hot embossing process. *J Micromech Microeng* **17**(12), 2420–2425.

Ishizawa, N., Idei, K., Kimura, T., Noda, D. & Hattori, T. (2008). Resin micromachining by roller hot embossing. *Microsyst Technol* **14**(9–11), 1381–1388.

Liu, S.-J., Huang, C.-C. & Liao, C.-T. (2012). Continuous infrared-assisted double-sided roll-to-roll embossing of flexible polymer substrates. *Polym Eng Sci* **52**(7), 1395–1401.

Lou, H., Li, W., Li, C. & Wang, X. (2013). Systematic investigation on parameters of solution blown micro/nanofibers using response surface methodology based on box-Behnken design. *J Appl Polym Sci* **130**(2), 1383–1391.

Metwally, K., Queste, S., Robert, L., Salut, R. & Khan-Malek, C. (2011). Hot roll embossing in thermoplastic foils using dry-etched silicon stamp and multiple passes. *Microelectron Eng* **88**(8), 2679–2682.

Myers, R.H., Montgomery, D.C. & Anderson-Cook, C.M. (2009). *Response Surface Methodology: Process and Product Optimization Using Designed Experiments*. Hoboken, NJ: Wiley.

Ng, S.H. & Wang, Z.F. (2008). Hot roller embossing for the creation of microfluidic devices. In *DTIP of MEMS and MOEMS—Symposium on Design, Test, Integration and Packaging of MEMS/MOEMS*, pp. 262–266. 9–11 April 2008, Nice, France. Grenoble, France: EDA Publishing.

Nouraei, S. & Roy, S. (2009). Design of experiments in electrochemical microfabrication. *Electrochimic Acta* **54**(9), 2444–2449.

Omar, F., Kolew, A., Brousseau, E.B. & Hirshy, H. (2013). Simulation and experimental study of the effects of process factors on the uniformity of the residual layer thickness in hot embossing. *J Micro Nano-Manuf* **1**(2), 021002.

Rowland, H.D., King, W.P., Sun, A.C. & Schunk, P.R. (2005*a*). Simulations of nonuniform embossing: The effect of asymmetric neighbor cavities on polymer flow during nanoimprint lithography. *J Vac Sci Technol B* **23**(6), 2958–2962.

Rowland, H.D., Sun, A.C., Schunk, P.R. & King, W.P. (2005*b*). Impact of polymer film thickness and cavity size on polymer flow during embossing: Toward process design rules for nanoimprint lithography. *J Micromech Microeng* **15**(12), 2414–2425.

Schift, H., Halbeisen, M., Schütz, U., Delahoche, B., Vogelsang, K. & Gobrecht, J. (2006). Surface structuring of textile fibers using roll embossing. *Microelectron Eng* **83**(4–9 Special Issue), 855–858.

Schulz, H., Wissen, M. & Scheer, H.-C. (2003). Local mass transport and its effect on global pattern replication during hot embossing. *Microelectron Eng* **67–68**(1), 657–663.

Shan, X., Jin, L., Soh, Y.C. & Lu, C.W. (2010). A polymer-metal hybrid flexible mould and application for large area hot roller embossing. *Microsyst Technol* **16**(8–9), 1393–1398.

Shan, X., Soh, Y.C., Shi, C.W.P., Tay, C.K. & Lu, C.W. (2008). Large area roller embossing of multilayered ceramic green composites. In *DTIP of MEMS and MOEMS—Symposium on Design, Test, Integration and Packaging of MEMS/MOEMS*, pp. 314–319. 9–11 April 2008, Nice, France. Grenoble, France: EDA Publishing.

Velten, T., Schuck, H., Haberer, W. & Bauerfeld, F. (2010). Investigations on reel-to-reel hot embossing. *Int J Adv Manuf Technol* **47**(1–4), 73–80.

Yeo, L.P., Ng, S.H., Wang, Z., Wang, Z. & de Rooij, N.F. (2009). Micro-fabrication of polymeric devices using hot roller embossing. *Microelectron Eng* **86**(4–6), 933–936.

Yeo, L.P., Ng, S.H., Wang, Z.F., Xia, H.M., Wang, Z.P., Thang, V.S., Zhong, Z.W. & Rooij, N.F.D. (2010). Investigation of hot roller embossing for microfluidic devices. *J Micromech Microeng* **20**(1), 015017.

Yun, D., Son, Y., Kyung, J., Park, H., Park, C., Lee, S. & Kim, B. (2012). Development of roll-to-roll hot embossing system with induction heater for micro fabrication. *Rev Sci Instrum* **83**(1), 015108.